Geometric phase corrected by initial system-environment correlations

Sharoon Austin, Sheraz Zahid, and Adam Zaman Chaudhry*

School of Science & Engineering, Lahore University of Management Sciences (LUMS), Opposite Sector U, D.H.A, Lahore 54792, Pakistan

(Received 2 September 2019; revised manuscript received 17 December 2019; accepted 4 February 2020; published 25 February 2020)

We find the geometric phase of a two-level system undergoing pure dephasing via interaction with an arbitrary environment, taking into account the effect of the initial system-environment correlations. We use our formalism to calculate the geometric phase for the two-level system in the presence of both harmonic-oscillator and spin environments, and we consider the initial state of the two-level system to be prepared by a projective measurement or a unitary operation. The geometric phase is evaluated for a variety of parameters such as the system-environment coupling strength to show that the initial correlations can affect the geometric phase very significantly even for weak and moderate system-environment coupling strengths. Moreover, the correction to the geometric phase due to the system-environment coupling generally becomes smaller (and can even be zero) if initial system-environment correlations are taken into account, thus implying that the system-environment correlations can increase the robustness of the geometric phase.

DOI: 10.1103/PhysRevA.101.022114

I. INTRODUCTION

The geometric phase is the phase information acquired by a system due to its cyclic evolution in a curved parameter space [1,2]. This phenomenon was first studied by Pancharatnam in optics [3] and by Longuet-Higgins [4] and Stone [5] in quantum chemistry. Berry's finding that the geometric phase arises generally in the study of closed quantum systems undergoing cyclic adiabatic evolutions ignited interest in the subject [6]. Aharonov and Anandan thereafter generalized the geometric phase to nonadiabatic evolutions, showing that the phase depends on the geometry of the path followed by the system in the projective Hilbert space [7], while Uhlmann considered the geometric phase for mixed quantum states [8] which was further generalized by Sjoqvist *et al.* [9]. On the experimental front, the geometric phase has been observed in nuclear magnetic resonance [10], superconducting [11], and optical setups [12], amongst others.

Besides its theoretical importance, the geometric phase has practical applications as well. For example, the geometric phase has been used as a tool to study many-body quantum systems in and out of equilibrium—see, for example, Refs. [13,14]. Moreover, due to its geometric nature, the geometric phase may have intrinsic resistance to external noise, which makes it an attractive tool for robust quantum information processing [15–20]. It is then important to extend the study of the geometric phase to open quantum systems where the effect of the environment on the geometric phase can be investigated. Different approaches have been used to investigate the effect of the environment on the geometric phase [21–34]. In particular, emphasis has been on a single two-level system undergoing pure dephasing, that is, it is assumed that dephasing plays a much more dominant role compared to relaxation effects. In this case, starting from a product state of the two-level system and the environment in thermal equilibrium, the density matrix of the two-level system can be computed as a function of time, and the geometric phase can then be obtained. Of particular importance to us is Ref. [32], where the effect of non-Markovianity on the geometric phase is studied. Given that memory effects can play a role, it is then natural to consider the effect of initial system-environment correlations on the geometric phase as well [35–65]. The effect of the initial correlations is expected to be especially significant if the system-environment coupling is not weak, since, in this case, the initial state can no longer be assumed to be a product state of the system and the environment thermal equilibrium state. Therefore, in this work, we aim to study the geometric phase for the pure dephasing model, taking the initial system-environment correlations into account.

We start by deriving general expressions for the geometric phase of a two-level system undergoing pure dephasing for both initially pure and mixed states. Our expressions are general in the sense that we do not make any assumptions regarding the form of the environment or the system-environment coupling, and they take the initial system-environment correlations into account. We then apply these expressions to two concrete well-known system-environment models: a two-level system undergoing dephasing via interaction with a harmonic-oscillator environment, and a two-level system undergoing pure dephasing due to a spin environment. Both of these models are exactly solvable for arbitrary system-environment coupling strengths even if initial system-environment correlations are taken into account. The initial state of the two-level system is prepared either by performing a projective measurement on the system only (the initial state of the system is pure in this case), or by performing a unitary operation on the system (the initial state is now, in general, mixed). Using the exact solutions, we investigate the effect of the initial

*adam.zaman@lums.edu.pk

system-environment correlations on the geometric phase as various physical parameters such as the system-environment coupling strength and the temperature are varied. We find that, in general, the initial correlations can affect the geometric phase very significantly, even for weak and moderate system-environment coupling strengths. Interestingly, the initial correlations can make the geometric phase more robust; in fact, the correction to the geometric phase due to the environment can become zero for specific values of system-environment parameters if the initial correlations are taken into account.

This paper is organized as follows. In Sec. II, we derive expressions for the geometric phase of a two-level system undergoing pure dephasing for both initially pure and mixed system states. In Sec. III, we compute the geometric phase for a two-level system interacting with an environment of harmonic oscillators both with and without initial system-environment correlations. A similar task is performed for a spin environment in Sec. IV. Finally, we summarize our results in Sec. V. Details regarding the solutions of the system-environment models employed are presented in the Appendixes.

II. FORMALISM

A. Pure initial system state

Consider a two-level system with Hamiltonian H_S interacting with an arbitrary environment whose Hamiltonian is H_B. The system-environment interaction is H_{SB}. The total system-environment Hamiltonian is then

$$H = H_S + H_B + H_{SB}. \tag{1}$$

For a pure dephasing model, $[H_S, H_{SB}] = 0$, which means that, in the eigenbasis of H_S, the diagonal elements of the density matrix of the two-level system do not change. In this basis, the initial state of the two-level system (assumed to be pure) can be written as

$$\rho(0) = \begin{bmatrix} \cos^2\left(\frac{\theta_0}{2}\right) & \frac{1}{2}\sin\theta_0 e^{-i\phi_0} \\ \frac{1}{2}\sin\theta_0 e^{i\phi_0} & \sin^2\left(\frac{\theta_0}{2}\right) \end{bmatrix}. \tag{2}$$

Here $0 \leqslant \theta_0 \leqslant \pi$, $0 \leqslant \phi_0 < 2\pi$ are the usual Bloch angles characterizing the initial system state. Since we are considering only pure dephasing, time evolution leads to a density matrix of the form

$$\rho(t) = \begin{bmatrix} \cos^2\left(\frac{\theta_0}{2}\right) & \frac{1}{2}\sin\theta_0 e^{-i\Omega(t)}e^{-\Gamma(t)} \\ \frac{1}{2}\sin\theta_0 e^{i\Omega(t)}e^{-\Gamma(t)} & \sin^2\left(\frac{\theta_0}{2}\right) \end{bmatrix}. \tag{3}$$

It is important to note that the density matrix $\rho(t)$ will have this form even in the presence of initial system-environment correlations—only the form of $\Omega(t)$ and $\Gamma(t)$ can be different. Now, in the Bloch vector representation, we can write $\rho(t)$ as

$$\rho(t) = \tfrac{1}{2}[\mathbb{1} + n_x\sigma_x + n_y\sigma_y + n_z\sigma_z],$$

where $n_x = \sin\theta_0 e^{-\Gamma(t)}\cos[\Omega(t)]$, $n_y = \sin\theta_0 e^{-\Gamma(t)}\sin[\Omega(t)]$, and $n_z = \cos\theta_0$. Given the density matrix $\rho(t)$, we can compute the geometric phase Φ_G via [23]

$$\Phi_G = \arg\left(\sum_{k=1}^{2}\sqrt{\varepsilon_k(0)\varepsilon_k(\tau)}\langle\varepsilon_k(0)|\varepsilon_k(\tau)\rangle e^{-\int_0^\tau dt\,\langle\varepsilon_k|\frac{\partial}{\partial t}|\varepsilon_k\rangle}\right). \tag{4}$$

Here $\varepsilon_k(t)$ are the eigenvalues of the density matrix $\rho(t)$, $|\varepsilon_k(t)\rangle$ are the eigenvectors, and τ is the time after which the system completes a cyclic evolution. This so-called kinematic approach to calculating the geometric phase essentially extracts, from the total phase picked up during the evolution, a purification independent part; this purification independent part is then labeled as the geometric phase since it is gauge invariant and reproduces the well-known results for closed quantum systems. Now, for our case, the eigenvalues of $\rho(t)$ are

$$\varepsilon_\pm(t) = \tfrac{1}{2}\left(1 \pm \sqrt{1 + \sin^2\theta_0[e^{-2\Gamma(t)} - 1]}\right). \tag{5}$$

Notice that the eigenvalues are independent of $\Omega(t)$. Moreover, since $\varepsilon_-(0) = 0$, as is expected for a pure initial system state, our calculation of the geometric phase greatly simplifies. The corresponding eigenvectors of $\rho(t)$ are

$$|\varepsilon_+(t)\rangle = \cos\left(\frac{\theta}{2}\right)|0\rangle + e^{i\Omega(t)}\sin\left(\frac{\theta}{2}\right)|1\rangle, \tag{6}$$

$$|\varepsilon_-(t)\rangle = \sin\left(\frac{\theta}{2}\right)|0\rangle - e^{i\Omega(t)}\cos\left(\frac{\theta}{2}\right)|1\rangle, \tag{7}$$

where

$$\sin\theta = \mathcal{F}(t)^{-1}\sin\theta_0 e^{-\Gamma(t)},$$
$$\cos\theta = \mathcal{F}(t)^{-1}\cos\theta_0,$$
$$\mathcal{F}(t) = \sqrt{1 + \sin^2\theta_0(e^{-2\Gamma(t)} - 1)},$$

and $|0\rangle$ and $|1\rangle$ are the eigenstates of H_S. Since $\varepsilon_-(0) = 0$,

$$\Phi_G = \arg\left(\sqrt{\varepsilon_+(0)\varepsilon_+(\tau)}\langle\varepsilon_+(0)|\varepsilon_+(\tau)\rangle e^{-\int_0^\tau dt\,\langle\varepsilon_+|\frac{\partial}{\partial t}|\varepsilon_+\rangle}\right).$$

This further simplifies to

$$\Phi_G = \arg\left(\langle\varepsilon_+(0)|\varepsilon_+(\tau)\rangle e^{-\int_0^\tau dt\,\langle\varepsilon_+|\frac{\partial}{\partial t}|\varepsilon_+\rangle}\right),$$

since $\sqrt{\varepsilon_+(0)\varepsilon_+(\tau)}$ is real. We also find that $\langle\varepsilon_+|\frac{\partial}{\partial t}|\varepsilon_+\rangle = i\dot{\Omega}\sin^2\left(\frac{\theta}{2}\right)$, where the dot denotes the time derivative. Moreover,

$$\langle\varepsilon_+(0)|\varepsilon_+(\tau)\rangle = \cos\left(\frac{\theta}{2}\right)\cos\left(\frac{\theta_0}{2}\right) + e^{i\Omega(\tau)}e^{-i\phi_0}\sin\left(\frac{\theta}{2}\right)\sin\left(\frac{\theta_0}{2}\right).$$

The geometric phase can then be written as

$$\Phi_G = \Phi_1 + \Phi_2, \tag{8}$$

with $\Phi_1 = -\int_0^\tau dt\,\dot{\Omega}\sin^2\left(\frac{\theta}{2}\right)$ and $\Phi_2 = \arg[1 + e^{i\Omega(\tau)}e^{-i\phi_0}\tan\left(\frac{\theta}{2}\right)\tan\left(\frac{\theta_0}{2}\right)]$. To evaluate each of these one by one, we first note that H_S has a characteristic frequency ω_0 such that $\omega_0\tau = 2\pi$. Then, $\Omega(t)$ can be written as $\Omega(t) = \phi_0 + \omega_0 t + \chi(t)$, where $\chi(t)$ takes into account part of the effect of the system-environment coupling. It follows that

$$\Phi_1 = -\int_0^\tau dt\,(\omega_0 + \dot{\chi})\sin^2\left(\frac{\theta}{2}\right),$$

which can be simplified to

$$\Phi_1 = -\pi - \frac{\chi(\tau)}{2} + \frac{\cos\theta_0}{2}I(\tau), \tag{9}$$

with

$$I(\tau) = \int_0^\tau \mathcal{F}(t)^{-1}[\omega_0 + \dot{\chi}(t)]\,dt.$$

As for Φ_2, we can write

$$\Phi_2 = \arg\left(1 + e^{i\chi(\tau)} \tan\left[\frac{\theta(0)}{2}\right] \tan\left[\frac{\theta(\tau)}{2}\right]\right).$$

Since $\tan\left(\frac{\theta}{2}\right) = \frac{\sin\theta}{1+\cos\theta}$ and $\tan\theta = (\tan\theta_0)e^{-\Gamma(t)}$, this further simplifies to

$$\Phi_2 = \arg\left(1 + e^{i\chi(\tau)} e^{-\Gamma(\tau)} \frac{1-\cos\theta_0}{\mathcal{F}(\tau) + \cos\theta_0}\right). \tag{10}$$

With Φ_1 and Φ_2 found, we can thereby calculate Φ_G. It should be noted that, if the system-environment interaction strength is zero, we find that $\Phi_1 = -\pi + \pi\cos\theta_0$ while $\Phi_2 = 0$, thereby leading to the usual result $\Phi_G = -\pi + \pi\cos\theta_0$ [7]. Moreover, for $\theta_0 = \pi/2$, $\Phi_1 = -\pi - \frac{\chi(\tau)}{2}$ and $\Phi_2 = \frac{\chi(\tau)}{2}$, meaning that $\Phi_G = -\pi$. Thus the geometric phase is robust for the states with $\theta_0 = \pi/2$ even if initial correlations are taken into account. Consequently, we will consider $\theta_0 \neq \pi/2$ to investigate the effect of the initial correlations on the geometric phase. Before doing so for concrete system-environment models, we generalize our results to the case where the initial state is mixed.

B. Mixed initial system state

We now derive expressions for the geometric phase for initially mixed states. Our approach will be to write the state for the two-level system in a form similar to that in Eqs. (2) and (3) so that we obtain an expression for the geometric phase similar to that in Eq. (8). As such, we start by noting that the initial density matrix, even for a mixed state, can be written as

$$\rho(0) = \begin{pmatrix} \cos^2\left(\frac{\tilde{\theta}_0}{2}\right) & \frac{1}{2}e^{-\Gamma_0}\sin\tilde{\theta}_0 e^{-i\phi_0} \\ \frac{1}{2}e^{-\Gamma_0}\sin\tilde{\theta}_0 e^{i\phi_0} & \sin^2\left(\frac{\tilde{\theta}_0}{2}\right). \end{pmatrix}. \tag{11}$$

Note that $\tilde{\theta}_0$ is not a Bloch angle here. $\Gamma_0 > 0$ takes into account that the initial state is mixed. It follows that

$$\rho(t) = \begin{pmatrix} \cos^2\left(\frac{\tilde{\theta}_0}{2}\right) & \frac{1}{2}\sin\tilde{\theta}_0 e^{-i\Omega(t)-\Gamma_0-\Gamma(t)} \\ \frac{1}{2}\sin\tilde{\theta}_0 e^{i\Omega(t)-\Gamma_0-\Gamma(t)} & \sin^2\left(\frac{\tilde{\theta}_0}{2}\right) \end{pmatrix},$$

with $\Omega(t) = \omega_0 t + \chi(t) + \phi_0$ as before. The eigenvalues of the density matrix $\rho(t)$ are now a simple extension of Eq. (5), that is,

$$\varepsilon_\pm = \tfrac{1}{2}(1 \pm \tilde{\mathcal{F}}(t)), \tag{12}$$

with

$$\tilde{\mathcal{F}}(t) = \sqrt{1 + \sin^2\tilde{\theta}_0(e^{-2\Gamma_0}e^{-2\Gamma(t)} - 1)}.$$

The corresponding eigenvectors are similarly

$$|\varepsilon_+\rangle = \cos\left(\frac{\tilde{\theta}}{2}\right)|0\rangle + e^{i\Omega(t)}\sin\left(\frac{\tilde{\theta}}{2}\right)|1\rangle,$$

$$|\varepsilon_-\rangle = \sin\left(\frac{\tilde{\theta}}{2}\right)|0\rangle - e^{i\Omega(t)}\cos\left(\frac{\tilde{\theta}}{2}\right)|1\rangle,$$

where $\sin\tilde{\theta} = \sin\tilde{\theta}_0 e^{-\Gamma_0}e^{-\Gamma(t)}\tilde{\mathcal{F}}(t)^{-1}$ and $\cos\tilde{\theta} = \cos\tilde{\theta}_0\,\tilde{\mathcal{F}}(t)^{-1}$. With the density matrix $\rho(t)$ found, the geometric phase Φ_G can be written as

$$\Phi_G = \Phi_1 + \Phi_2 + \Phi_3, \tag{13}$$

with

$$\Phi_1 = \arg\left(e^{-\int_0^\tau dt\,\langle\varepsilon_+|\frac{\partial}{\partial t}|\varepsilon_+\rangle}\right),$$

$$\Phi_2 = \arg\langle\varepsilon_+(0)|\varepsilon_+(\tau)\rangle,$$

$$\Phi_3 = \arg\left(1 + \sqrt{\frac{\varepsilon_-(0)\varepsilon_-(\tau)}{\varepsilon_+(0)\varepsilon_+(\tau)}}\frac{\langle\varepsilon_-(0)|\varepsilon_-(\tau)\rangle}{\langle\varepsilon_+(0)|\varepsilon_+(\tau)\rangle} \times e^{\int_0^\tau dt\,\langle\varepsilon_+|\frac{\partial}{\partial t}|\varepsilon_+\rangle - \langle\varepsilon_-|\frac{\partial}{\partial t}|\varepsilon_-\rangle}\right).$$

The calculations for Φ_1 and Φ_2 can be performed as done before to obtain

$$\Phi_1 = -\pi - \frac{\chi(\tau)}{2} + \frac{1}{2}\cos\tilde{\theta}_0\tilde{I}(\tau), \tag{14}$$

where

$$\tilde{I}(\tau) = \int_0^\tau dt\,\frac{\omega_0 + \dot{\chi}}{\sqrt{1 + \sin^2\tilde{\theta}_0(e^{-2\Gamma_0}e^{-2\Gamma(t)} - 1)}}$$

and

$$\Phi_2 = \arg\left(1 + e^{i\chi(\tau)}\tan\left[\frac{\tilde{\theta}(0)}{2}\right]\tan\left[\frac{\tilde{\theta}(\tau)}{2}\right]\right). \tag{15}$$

Finally, we compute Φ_3 and find that

$$\Phi_3 = \arg(1 + a(\tau)b(\tau)e^{-i\cos\tilde{\theta}_0\tilde{I}(\tau)}), \tag{16}$$

where

$$a(\tau) = \sqrt{\frac{\varepsilon_-(0)\varepsilon_-(\tau)}{\varepsilon_+(0)\varepsilon_+(\tau)}}$$

and

$$b(\tau) = \frac{\tan\left[\frac{\tilde{\theta}(0)}{2}\right]\tan\left[\frac{\tilde{\theta}(\tau)}{2}\right] + e^{i\chi(\tau)}}{1 + e^{i\chi(\tau)}\tan\left[\frac{\tilde{\theta}(0)}{2}\right]\tan\left[\frac{\tilde{\theta}(\tau)}{2}\right]}.$$

Finding the geometric phase now is simply a matter of finding the parameters $\tilde{\theta}_0$, ϕ_0, and Γ_0 characterizing the initial state as well as the functions $\Gamma(t)$ and $\chi(t)$ that go into the time evolution of the system density matrix. It is important to realize that if the system-environment interaction is zero, the geometric phase is, in general, no longer $-\pi + \pi\cos\tilde{\theta}_0$, since the initial state is mixed. However, for $\tilde{\theta}_0 = \pi/2$, we again obtain $\Phi_G = -\pi$.

We will now use the expressions for the geometric phase to perform calculations with concrete system-environment models, both with and without initial system-environment correlations.

III. TWO-LEVEL SYSTEM INTERACTING WITH AN ENVIRONMENT OF HARMONIC OSCILLATORS

We first apply our formalism to the paradigmatic example of a single two-level system undergoing pure dephasing via interaction with a collection of harmonic oscillators [66]. The total system-environment Hamiltonian is $H = H_S + H_B + H_{SB}$, where (we set $\hbar = 1$ throughout)

$$H_S = \frac{\omega_0}{2}\sigma_z, \quad H_B = \sum_k \omega_k b_k^\dagger b_k,$$
$$H_{SB} = \sigma_z \sum_k (g_k^* b_k + g_k b_k^\dagger),$$

and σ_z is the usual Pauli matrix, ω_0 is the energy bias, and b_k ($b_k^\dagger$) are the annihilation (creation) operators for the harmonic-oscillator modes. Since $[H_S, H_{SB}] = 0$, $\langle\sigma_z\rangle$ does not change with time, and only dephasing takes place. Assuming that the initial system-environment state is a product state with the environment in a thermal equilibrium state $\rho_B = e^{-\beta H_B}/Z_B$, where $Z_B = \text{Tr}_B[e^{-\beta H_B}]$, the evolution of the off-diagonal elements of the density matrix is given by [66]

$$\langle\sigma_\pm(t)\rangle = \langle\sigma_\pm\rangle e^{\pm i\omega_0 t} e^{-\Gamma_{\text{uc}}(t)}, \tag{17}$$

where

$$\Gamma_{\text{uc}}(t) = \sum_k 4|g_k|^2 \coth(\beta\omega_k/2)\frac{1-\cos\omega_k t}{\omega_k^2}.$$

For completeness, the derivation of this result is presented in Appendix A. On the other hand, if the system and the environment have interacted for a long time beforehand, the initial state of the environment is not the thermal equilibrium state $e^{-\beta H_B}/Z_B$. Instead, the system and the environment together are in a thermal equilibrium state, that is, $e^{-\beta H}/Z$, where $Z = \text{Tr}_{S,B}[e^{-\beta H}]$ [67]. Then, at time $t = 0$, we can perform either a projective measurement or a unitary operation on the system to prepare the desired initial system state. We now analyze these scenarios one by one.

A. System state preparation by projective measurement

If the initial system state $|\psi\rangle$ is prepared by a projective measurement, described by the projector $P_\psi = |\psi\rangle\langle\psi|$, then the initial system-environment state is $\rho(0) = \frac{1}{Z}P_\psi e^{-\beta H}P_\psi$ with $Z = \text{Tr}_{S,B}[P_\psi e^{-\beta H}]$. With this initial state, the evolution of the off-diagonal elements of the system density matrix is given by [53,55]

$$\langle\sigma_\pm(t)\rangle = \langle\sigma_\pm\rangle e^{\pm i[\omega_0 t + \chi(t)]} e^{-\Gamma(t)}, \tag{18}$$

where

$$\Gamma(t) = \Gamma_{\text{uc}}(t) + \Gamma_{\text{corr}}(t),$$

$$\Gamma_{\text{corr}}(t) = -\frac{1}{2}\ln\left[1 - \frac{(1-\cos^2\theta_0)\sin^2[\Phi(t)]}{[\cosh(\beta\omega_0/2) - \cos\theta_0\sinh(\beta\omega_0/2)]^2}\right],$$

$$\tan[\chi(t)] = \frac{\sinh(\beta\omega_0/2) - \cos\theta_0\cosh(\beta\omega_0/2)}{\cosh(\beta\omega_0/2) - \cos\theta_0\sinh(\beta\omega_0/2)}\tan[\Phi(t)],$$

$$\Phi(t) = \sum_k \frac{4|g_k|^2}{\omega_k^2}\sin(\omega_k t).$$

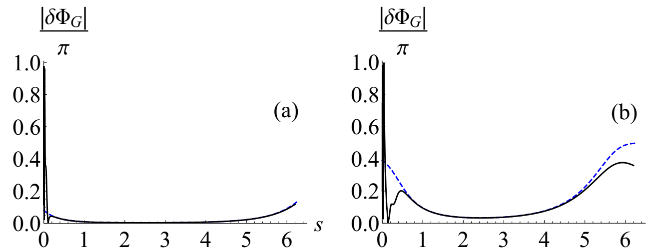

FIG. 1. Correction to the geometric phase $\delta\Phi_G \equiv \Phi_G - \Phi_U$ (where $\Phi_U = -\pi + \pi\cos\theta_0$) of the two-level system in the presence of the harmonic-oscillator environment as a function of the Ohmicity parameter s for weak system-environment coupling strength. The solid, black curve shows the geometric phase when the initial state is prepared via a projective measurement, while the dashed, blue curve is for an uncorrelated initial state [that is, the dynamics are given by Eq. (17)]. In (a), the system-environment coupling strength is $\lambda = 0.01$, while in (b) we have used $\lambda = 0.1$. Throughout, we are working in dimensionless units with $\hbar = 1$, and here we have set $\omega_0 = 1$. We have used $\omega_c = 5$, $\theta_0 = \pi/3$, and $\beta = \frac{1}{k_B T} \to \infty$ (zero temperature). Correspondingly, the thermal correlation time $t_B = \beta/\pi \to \infty$, and the cutoff time $t_c = 1/\omega_c = 0.2$. Throughout the paper, $\tau > t_B$ and $\tau > t_c$. Also, for $s = 1$, $\Gamma(\tau) \approx 0.34$ for $\lambda = 0.1$, which means that the coherences are still very significant at time τ.

For completeness, the derivation of these results is sketched in Appendix A. Note that the effect of the initial correlations is to modify the decoherence rate as well as to introduce a phase shift $\chi(t)$. This phase shift arises because the initial state of the environment is no longer a thermal state of harmonic oscillators in equilibrium; rather, the initial state of the environment consists of a collection of displaced harmonic oscillators, as can be seen mathematically in Appendix A in detail. These displaced harmonic oscillators not only decohere the central spin, but also "produce" an effective "magnetic" field for the central spin given by $B(t) = \frac{d\chi}{dt}$. For zero temperature, these expressions further simplify to $\Gamma_{\text{corr}}(t) = 0$, meaning that the displaced harmonic oscillators lead to the same decoherence rate as the usual thermal equilibrium bath of harmonic oscillators, and $\chi(t) = \Phi(t)$. These facts will be useful in our discussion of the behavior of the geometric phase below.

With the system density matrix found, the geometric phase can now be evaluated. To calculate the sum over the environment modes, the sum is converted to an integral via the spectral density $J(\omega)$, which allows us to write $\sum_k 4|g_k|^2(\ldots)$ as $\int_0^\infty d\omega\, J(\omega)(\ldots)$. We consider the spectral density to be of the form $J(\omega) = \lambda\omega^s\omega_c^{1-s}e^{-\omega/\omega_c}$, where λ is a dimensionless constant characterizing the system-environment interaction strength, s is the so-called Ohmicity parameter, and ω_c is the cutoff frequency [66]. With this form of the spectral density, Γ_{uc} and $\Phi(t)$ can be found analytically—the expressions are given in Appendix A. In Figs. 1(a) and 1(b), we have plotted the behavior of the correction to the geometric phase $|\delta\Phi_G| = |\Phi_G - \Phi_U|$ (where Φ_U is the geometric phase when the system-environment coupling strength is zero), as the Ohmicity parameter is varied for weak system-environment coupling strength. It is clear from these figures that, for weak

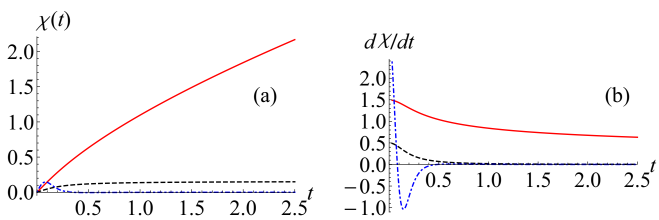

FIG. 2. Phase shift $\chi(t)$ [see (a)] and the effective magnetic field $\frac{d\chi}{dt} = B(t)$ [see (b)] as a function of time for different Ohmicities s. The solid red curve is with $s = 0.3$, and the black dashed and the blue dot-dashed curves are with $s = 1$ and $s = 4$, respectively. Throughout, we are working in dimensionless units with $\hbar = 1$, and here we have set $\omega_0 = 1$. We have used $\lambda = 0.1$, $\omega_c = 5$, $\theta_0 = \pi/3$, and $\beta \to \infty$ (zero temperature).

system-environment coupling strength, the effect of the initial correlations on the geometric phase is generally negligible since the dashed blue line largely overlaps with the solid black curve. Nevertheless, for sub-Ohmic environments (that is, $s < 1$), the initial correlations can still play a role. Interestingly, taking the initial correlations into account generally makes the correction to the geometric phase smaller. In fact, for a particular value of the Ohmicity parameter, the correction to the geometric phase is zero.

Let us now analyze these results in detail. As mentioned before, the initial state of the environment when the system-environment interaction is taken into account consists of displaced harmonic oscillators. These displaced harmonic oscillators lead to not only the decoherence of the central system, but also a phase shift $\chi(t)$. At zero temperature, this phase shift is given by $\chi(t) = \int_0^\infty d\omega \frac{J(\omega)}{\omega^2}\sin(\omega t)$ (see Appendix A). The form of this phase shift implies that the effective "magnetic" field [defined as $B(t) = \frac{d\chi}{dt}$] due to the system-environment correlations is $B(t) = \int_0^\infty d\omega \frac{J(\omega)}{\omega}\cos(\omega t)$. For sub-Ohmic environments, this effective magnetic field will clearly be very significant. To be more quantitative, with $J(\omega) = \lambda\omega^s\omega_c^{1-s}e^{-\omega/\omega_c}$, it is found that

$$\chi(t) = \frac{\lambda\Gamma(s-1)}{\left(1+\omega_c^2t^2\right)^{(s-1)/2}}\sin[(s-1)\tan^{-1}(\omega_c t)], \qquad (19)$$

if $s \neq 1$, while $\chi(t) = \lambda \tan^{-1}(\omega_c t)$ for $s = 1$. Behavior of this phase shift for different values of s is illustrated in Fig. 2. For Ohmic environments, the effective magnetic field is initially nonzero, but quickly decays to zero. For super-Ohmic environments, the effective magnetic field is initially very large; it then quickly decreases, flips direction, and decays to zero. On the other hand, for sub-Ohmic environments, the effective magnetic field remains nonzero even at long times. In fact, for extreme sub-Ohmic environments, we can show that the phase shift is approximately $\chi(t) \approx -\lambda\Gamma(s-1)\omega_c t$, which means that the displaced harmonic oscillators lead to an approximately constant effective magnetic field $B(t) = -\lambda\Gamma(s-1)\omega_c$. The fact that this magnetic field is approximately constant can simply be understood as a manifestation of the fact that the sub-Ohmic case is dominated by very low frequency harmonic oscillators. Now, the key point is that this effective magnetic field leads to an additional contribution to

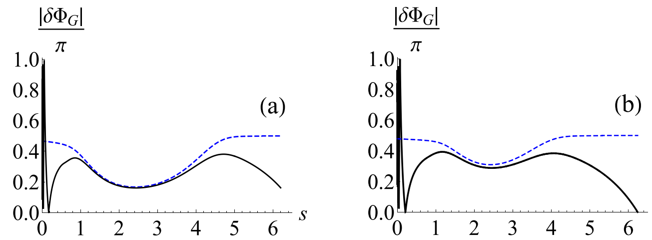

FIG. 3. Same as Fig. 1 except that in (a) we have $\lambda = 0.5$ and in (b) we have $\lambda = 1$.

the geometric phase, which can in fact cancel the correction to the geometric phase due to decoherence, meaning that we are only left with the unitary contribution to the geometric phase. To see this more clearly, let us recall that we have written $\Phi_G = \Phi_1 + \Phi_2$, where Φ_1 and Φ_2 are given by Eqs. (9) and (10). To discuss the effect of the system-environment correlations in a more transparent manner, we rewrite the geometric phase as

$$\Phi_G = \Phi_U + [G_2(\tau) - G_1(\tau)] + \Phi_2, \qquad (20)$$

where

$$G_1(\tau) = \frac{\chi(\tau)}{2} - \frac{\cos\theta_0}{2}K(\tau), \qquad (21)$$

$$G_2(\tau) = \frac{\cos\theta_0}{2}D(\tau) - \pi\cos\theta_0, \qquad (22)$$

with $D(\tau) = \int_0^\tau \frac{\omega_0}{F(t)}dt$ and $K(\tau) = \int_0^\tau \frac{B(t)}{F(t)}dt$. Note that here $\Phi_U = -\pi + \pi\cos\theta_0$ is the contribution to the geometric phase due to the unitary evolution. In the absence of system-environment correlations, we simply have $\Phi_G = \Phi_U + G_2(\tau)$; the fact that we are dealing instead with an environment of displaced harmonic oscillators adds in the additional corrections $G_1(\tau)$ and Φ_2. The first point to note is that for weak coupling, $\chi(\tau)$ is small, while for stronger coupling, $\Gamma(\tau)$ is significant. This implies that, in either case, Φ_2 is very small, which means that we can ignore this term in the following discussion. Now, recalling that $\mathcal{F}(t) = \sqrt{1+\sin^2\theta_0(e^{-2\Gamma(t)}-1)}$, and assuming for simplicity that $0 \leqslant \theta_0 < \frac{\pi}{2}$, it is clear that $\cos\theta_0 < \mathcal{F}(t) \leqslant 1$ since $\Gamma(t) \geqslant 0$. Consequently, since $D(\tau) = \int_0^\tau \frac{\omega_0}{\mathcal{F}(t)}dt$, $2\pi \leqslant D(\tau) < \frac{2\pi}{\cos\theta_0}$, which immediately implies that $\pi\cos\theta_0 \leqslant \frac{D(\tau)}{2}\cos\theta_0 < \pi$. Thus $0 \leqslant G_2(\tau) < \pi - \pi\cos\theta_0$. In other words, $G_2(\tau)$ is always positive definite and its maximum value is $-\Phi_U$. This is true for any environment. On the other hand, given the expression for $\chi(t)$ in Eq. (19), we find that, for sub-Ohmic environments, $B(t) \geqslant 0$. We can then derive in a similar manner that $\frac{\chi(\tau)}{2}\cos\theta_0 \leqslant \frac{K(\tau)}{2}\cos\theta_0 < \frac{\chi(\tau)}{2}$, which means that, for sub-Ohmic environments, $G_1(\tau) \geqslant 0$. Thus, for sub-Ohmic environments, the effective magnetic field produced by the displaced harmonic oscillators can offset the effect of the correction to the geometric phase due to decoherence. Indeed, this effect can be understood in terms of a "toy" model, where an additional magnetic field acting on the two-level system is added in from the start and the initial system-environment state is the usual product state (see Appendix B).

Proceeding along similar lines, in Figs. 3(a) and 3(b) we have shown the correction to the geometric phase at

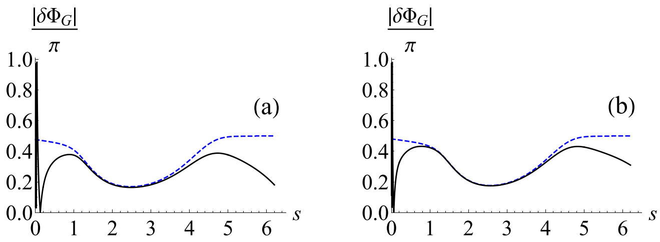

FIG. 4. Same as Fig. 1, except that the system-environment coupling strength is $\lambda = 0.5$, and in (a) we have $\beta = 2$ (therefore, $t_B = 2/\pi$), while in (b) we have $\beta = 1$ (corresponding to $t_B = 1/\pi$).

zero temperature for stronger system-environment coupling strengths. Three points are evident from these figures. First, for a range of values of s, the initial correlations have a very small effect on the geometric phase. In other words, $G_1(\tau)$ is small. Put simply, the effective magnetic field produced by the displaced oscillators is small, leading to the very small corrections. Second, for sub-Ohmic environments as well as for very super-Ohmic environments, the contribution of the initial correlations to the geometric phase is very significant. We have already discussed that, with sub-Ohmic environments, the displaced harmonic oscillators produce a slowly varying, almost constant, effective magnetic field which leads to a significant contribution to the geometric phase. For extreme super-Ohmic environments, on the other hand, we first note that decoherence becomes significant, meaning that $D(\tau)$ starts to approach its maximum value. Consequently, Φ_G becomes small in the absence of initial correlations. On the other hand, $K(\tau)$ depends on the history of the effective magnetic field produced by the displaced harmonic oscillators. While the effective magnetic field quickly becomes negligible for extreme super-Ohmic environments, it is nevertheless very significant at short times after the projective measurement (see Fig. 2), and this is precisely what makes $G_1(\tau)$ significant. Indeed, for a particular value of the Ohmicity parameter, this effective magnetic field produces a correction to the geometric phase that cancels precisely the contribution due to decoherence, that is, $G_2(\tau)$. As before, we can again understand this in terms of a toy model where an oscillating and decaying magnetic field is added in from the start (see Appendix B). To sum up, we have seen that the initial correlations generally reduce the correction to the geometric phase since, for both sub-Ohmic and extreme super-Ohmic environments, $G_1(\tau)$ can offset the correction due to $G_2(\tau)$. Let us also note that, as the temperature is increased, the effect of the initial correlations decreases, as expected [see Figs. 4(a) and 4(b)].

It is also interesting to analyze the correction to the geometric phase as the system-environment coupling strength is varied. As the coupling is increased, the harmonic oscillators are displaced more, leading to larger effective magnetic fields; however, the decoherence rate is also increased. The results are illustrated in Figs. 5(a) and 5(b). For the sub-Ohmic environment considered in Fig. 5(a), the initial correlations greatly reduce the correction to the geometric phase. As the system-environment coupling strength is increased, the correction to the geometric phase, in the case where the initial correlations are taken into account, can decrease. In fact, for particular nonzero values of the system-environment interaction strength, the correction to the geometric phase becomes zero—this is essentially the point where $G_1(\tau)$ becomes approximately equal to $G_2(\tau)$. This is not the case for an Ohmic environment [see Fig. 5(b)], simply because the effective magnetic field in this case is too small to offset the effect of decoherence.

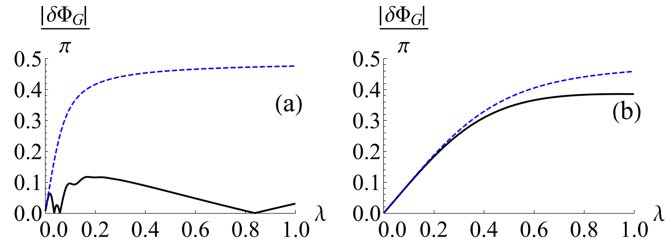

FIG. 5. Correction to the geometric phase $\delta\Phi_G \equiv \Phi_G - \Phi_U$ (where $\Phi_U = -\pi + \pi\cos\theta_0$) with a harmonic-oscillator environment as a function of the system-environment coupling strength λ. The solid, black curve shows the geometric phase when the initial state is prepared via a projective measurement, while the dashed, blue curve is for an uncorrelated initial state. In (a), the Ohmicity parameters are $s = 0.2$, while for (b) $s = 1$. These results are obtained for $\beta \to \infty$ (zero temperature). As before, we have set $\omega_0 = 1$, and we have used $\omega_c = 5$ and $\theta_0 = \pi/3$.

B. System state preparation by unitary operation

We now analyze the effect of the initial correlations if a unitary operation, instead of a projective measurement, is used to prepare the initial system state. The initial system-environment state in this case is $\rho(0) = \frac{1}{Z}\Omega\, e^{-\beta H}\Omega^\dagger$, where Ω is a unitary operation performed on the system. The off-diagonal elements of the system density matrix are given by [53,55]

$$\langle\sigma_\pm(t)\rangle = \langle\sigma_\pm(0)\rangle e^{\pm i[\omega_0 t + \chi(t)]}e^{-\Gamma(t)}, \tag{23}$$

with

$$\Gamma(t) = \Gamma_{\rm uc}(t) + \Gamma_{\rm corr}(t), \tag{24}$$

where

$$\Gamma_{\rm corr}(t) = -\ln\left\{\text{abs}\left[\frac{e^{-\beta\omega_0/2}\langle 0|\Omega^\dagger\sigma_+\Omega|0\rangle e^{-i\Phi(t)} + e^{\beta\omega_0/2}\langle 1|\Omega^\dagger\sigma_+\Omega|1\rangle e^{+i\Phi(t)}}{e^{-\beta\omega_0/2}\langle 0|\Omega^\dagger\sigma_+\Omega|0\rangle + e^{\beta\omega_0/2}\langle 1|\Omega^\dagger\sigma_+\Omega|1\rangle}\right]\right\}, \tag{25}$$

$$\chi(t) = \arg\left[\cos[\Phi(t)] + i\,\sin[\Phi(t)]\left(\frac{\langle 1|\Omega^\dagger\sigma_+\Omega|1\rangle e^{\beta\omega_0/2} - \langle 0|\Omega^\dagger\sigma_+\Omega|0\rangle e^{-\beta\omega_0/2}}{\langle 1|\Omega^\dagger\sigma_+\Omega|1\rangle e^{\beta\omega_0/2} + \langle 0|\Omega^\dagger\sigma_+\Omega|0\rangle e^{-\beta\omega_0/2}}\right)\right]. \tag{26}$$

Here $|0\rangle$ and $|1\rangle$ are the eigenstates of σ_z with $\sigma_z|l\rangle = (-1)^l|l\rangle$. These derivations are again sketched in Appendix A. One can check from these expressions that, for zero temperature, $\Gamma_{\text{corr}} = 0$ and $\chi(t) = \Phi(t)$. Consequently, the behavior of the geometric phase at zero temperature is the same as when the initial system state is prepared via a projective measurement. However, there will be differences at nonzero temperatures. The correction to the geometric phase $\delta\Phi_G = \Phi_G - \Phi_0$, where Φ_0 is the geometric phase for the two-level system if the system-environment coupling strength is zero, is plotted as a function of the Ohmicity parameter s for two different temperatures in Fig. 6 for moderate system-environment coupling strength. Once again, it is clear that the initial correlations can play a very significant role for the geometric phase, especially for sub-Ohmic environments.

IV. TWO-LEVEL SYSTEM INTERACTING WITH SPIN ENVIRONMENT

We now consider the central two-level system to be interacting with a collection of N two-level systems [68–71]. The system Hamiltonian H_S is still $\frac{\omega_0}{2}\sigma_z$, while the environment Hamiltonian is now $\sum_i \omega_i\sigma_x^i$, and the system-environment interaction is described by $\sigma_z\sum_i \lambda_i\sigma_z^i$. Since $[H_S, H_{SB}] = 0$, this is also a pure dephasing model. If the initial system-environment state is a product state of the form $\rho(0) = \rho_S(0)\otimes e^{-\beta H_B}/Z_B$, then the evolution of the off-diagonal elements is given by [69,71]

$$\langle\sigma_\pm(t)\rangle = \langle\sigma_\pm\rangle e^{\pm i\omega_0 t}e^{-\Gamma_{\text{uc}}(t)},$$

where

$$\Gamma_{\text{uc}}(t) = -\sum_j \ln\left\{1 - \frac{2\lambda_j^2}{\lambda_j^2+\omega_j^2}\sin^2\left(\sqrt{\lambda_j^2+\omega_j^2}\,t\right)\right\}$$

and the sum is over the environment spins. The derivation of this result is reproduced in Appendix C. However, as emphasized before, this result may be questionable since the initial system-environment correlations are disregarded. To investigate the effect of these correlations, we consider the system state to be prepared by a projective measurement as well as by a unitary operation starting from the total system-environment equilibrium state $e^{-\beta H}/Z$.

A. System state preparation by projective measurement

If the initial state is $\rho(0) = P_\psi e^{-\beta H}P_\psi/Z$, then the off-diagonal elements of the density matrix are given by

$$\langle\sigma_\pm(t)\rangle = \langle\sigma_\pm\rangle e^{\pm i[\omega_0 t+\chi(t)]}e^{-\Gamma(t)}, \tag{27}$$

where, similar to the form obtained for the harmonic-oscillator environment,

$$\tan[\chi(t)] = \frac{\sinh(\beta\omega_0/2) - \cos\theta_0\cosh(\beta\omega_0/2)}{\cosh(\beta\omega_0/2) - \cos\theta_0\sinh(\beta\omega_0/2)}\tan[\Phi(t)],$$

with θ_0 the Bloch angle characterizing the initial state. We now have

$$\Phi(t) = \sum_j \arg[A_j(t) + iB_j(t)], \tag{28}$$

where $A_j(t) = 1 - 2\frac{\lambda_j^2}{\alpha_{j^2}}\sin^2(\alpha_j t)$ and $B_j(t) = \frac{\lambda_j^2}{\alpha_j^2}\tanh(\beta\alpha_j)\sin(2\alpha_j t)$, with $\alpha_j = \sqrt{\lambda_j^2+\omega_j^2}$. Also, $\Gamma(t) = \Gamma_{\text{uc}}(t) + \Gamma_{\text{corr}}(t)$, where $\Gamma_{\text{corr}}(t) = \Gamma_{\text{corr}}^{(1)}(t) + \Gamma_{\text{corr}}^{(2)}(t)$, and

$$\Gamma_{\text{corr}}^{(1)}(t) = -\frac{1}{2}\sum_j \ln\left[1+(\lambda_j/\omega_j)^4\left(\frac{\tanh(\beta\alpha_j)\sin(2\alpha_j t)}{1+(\lambda_j/\omega_j)^2\cos(2\alpha_j t)}\right)^2\right], \tag{29}$$

$$\Gamma_{\text{corr}}^{(2)}(t) = -\frac{1}{2}\ln\left[1 - \frac{(1-\cos^2\theta_0)\sin^2[\Phi(t)]}{[\cosh(\beta\omega_0/2) - \cos\theta_0\sinh(\beta\omega_0/2)]^2}\right]. \tag{30}$$

Interestingly, in this case, even if the temperature is zero, the initial correlations change the decay rate of the off-diagonal elements since $\Gamma_{\text{corr}}^{(1)}(t) \neq 0$ at zero temperature, while $\Gamma_{\text{corr}}^{(2)}(t) = 0$. On the other hand, at zero temperature, $\chi(t)$ is once again equal to $\Phi(t)$.

With the system density matrix found, we compute the correction to the geometric phase $\delta\Phi_G = \Phi_G - \Phi_U$. The behavior of the correction $\delta\Phi_G$ as a function of the two-level system-environment coupling strength is shown in Figs. 7(a) and 7(b). The effect of the initial correlations is again very significant; in particular, the initial correlations can make the geometric phase more robust. For particular values of the system-environment interaction strength λ, the correction to the geometric phase becomes zero. As with the harmonic-oscillator environment, it is interesting to examine the physical reason behind the change in the geometric phase once the initial correlations are taken into account. Recall that for the harmonic-oscillator environment, the geometric phase is different precisely because, when the system-environment interaction is taken into account, the initial state of the environment consists of a collection of displaced harmonic oscillators rather than the usual environment of undisturbed

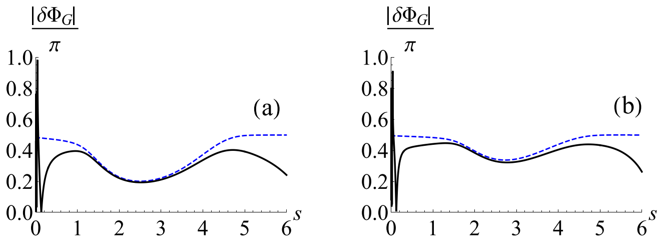

FIG. 6. Correction to the geometric phase $\delta\Phi_G \equiv \Phi_G - \Phi_0$ (where Φ_0 is the geometric phase for the two-level system if the system-environment interaction strength is zero) with a harmonic-oscillator environment as a function of the Ohmicity parameter s if the initial state is prepared via a unitary operation. The solid, black curve shows the geometric phase when the initial state is prepared via the unitary operation $\Omega = e^{i\pi\sigma_y/3}$, while the dashed, blue curve is for an uncorrelated initial state. In (a), we have $\beta = 3$ while in (b) we have $\beta = 1$. Once again, we have set $\omega_0 = 1$, and we have used $\omega_c = 5$ and $\lambda = 0.5$.

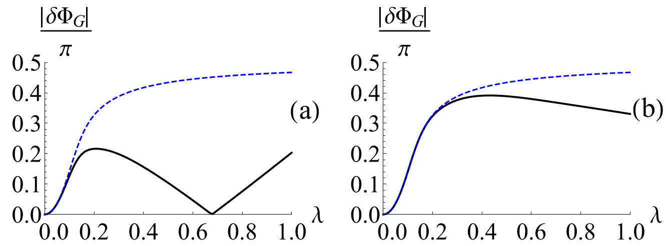

FIG. 7. Behavior of the correction to the geometric phase $\delta\Phi_G = \Phi_G - \Phi_U$ [here $\Phi_U = \pi(\cos\theta_0 - 1)$] as the spin-spin environment coupling strength λ is varied, both with (solid, black) and without (dashed, blue) initial correlations when the initial state is prepared via a projective measurement. We have considered the environment to be a spin bath with $N = 50$ and, for simplicity, we have assumed that the interaction strength between the central spin and each environment spin is the same (that is, $\lambda_j = \lambda$ for all j). As always, we are working in dimensionless units with $\hbar = 1$ and here have set $\omega_i = 1$ for all i. In (a), we have used zero temperature ($\beta \to \infty$), while in (b) $\beta = 0.4$. Also, $\omega_0 = 5$ and $\theta_0 = \pi/3$.

harmonic oscillators in equilibrium. The reason is similar for spin environments. A simple calculation shows that if the initial system-environment state is the usual product state, the initial state of the jth environment spin is specified by $\langle\sigma_x^j\rangle = -\tanh(\beta\omega_j)$ and $\langle\sigma_y^j\rangle = \langle\sigma_z^j\rangle = 0$. On the other hand, for the initial system-environment state $e^{-\beta H}/Z$, the state of the jth environment spin is given by $\langle\sigma_x^j\rangle = -\tanh(\beta\alpha_j)\frac{\omega_j}{\alpha_j}$, $\langle\sigma_y^j\rangle = 0$, and $\langle\sigma_z^j\rangle = \tanh(\beta\alpha_j)\tanh(\beta\omega_0/2)\frac{\lambda_j}{\alpha_j}$. Clearly, the Bloch vector of the jth now has a z component as well. As before, the effect of this different initial environment state is to produce a phase shift for the central two-level system, and this phase shift is what changes the geometric phase.

B. System state preparation by unitary operation

We now prepare the initial system state via a unitary operation. We find that for the initial system-environment state $\rho(0) = \frac{1}{Z}\Omega\, e^{-\beta H}\Omega^\dagger$, the off-diagonal elements of the density matrix are, as for the harmonic-oscillator environment,

$$\langle\sigma_\pm(t)\rangle = \langle\sigma_\pm(0)\rangle e^{\pm i[\omega_0 t + \chi(t)]}e^{-\Gamma(t)}, \tag{31}$$

where $\Gamma(t) = \Gamma_{\rm uc}(t) + \Gamma^{(1)}_{\rm corr}(t) + \Gamma^{(2)}_{\rm corr}(t)$ with $\Gamma^{(1)}_{\rm corr}(t)$ the same as before [see Eq. (29)], while $\Gamma^{(2)}_{\rm corr}(t)$ is given by

$$\Gamma^{(2)}_{\rm corr}(t) = -\ln\left\{{\rm abs}\left[\frac{e^{-\beta\omega_0/2}\langle 0|\Omega^\dagger\sigma_+\Omega|0\rangle e^{-i\Phi(t)} + e^{\beta\omega_0/2}\langle 1|\Omega^\dagger\sigma_+\Omega|1\rangle e^{i\Phi(t)}}{e^{-\beta\omega_0/2}\langle 0|\Omega^\dagger\sigma_+\Omega|0\rangle + e^{\beta\omega_0/2}\langle 1|\Omega^\dagger\sigma_+\Omega|1\rangle}\right]\right\}.$$

Also, $\chi(t)$ is of the same form as in Eq. (26), but with $\Phi(t)$ now given by Eq. (28). Details can be found in Appendix C. Once again, for zero temperature, we find that the dynamics are the same as the case where the initial state is prepared by a projective measurement. However, as illustrated in Figs. 8(a) and 8(b), even for nonzero temperatures, the contribution to the geometric phase due to the initial correlations can be very significant. Once again, if we increase the temperature, the effect of the initial correlations decreases as expected.

V. CONCLUSION

In summary, we have presented exact expressions for the geometric phase of a two-level system undergoing pure dephasing to investigate the effect of the initial system-environment correlations on the geometric phase. As concrete examples, we have applied these expressions to two different environments: a collection of harmonic oscillators and a collection of spins. Our results illustrate that the effect of the initial correlations on the geometric phase can be very significant, with a nontrivial dependence on the system-environment parameters. For instance, increasing the system-environment coupling strength may not always increase the correction to the geometric phase; in fact, for certain values of the coupling strength, the correction becomes zero, implying that the initial correlations can increase the robustness of the geometric phase. This increase in the robustness of the geometric phase has been shown to come about because, once the system-environment interaction before the system state preparation is taken into account, the initial state of the environment is different. Namely, for harmonic-oscillator environments, the initial state consists of a collection of displaced harmonic oscillators, while for the spin environment, the polarization of the environment spins changes due to the system-environment interaction. These different environment states then "produce" an effective "magnetic" field for the central two-level system. The additional correction to the geometric phase due to this effective field can cancel the correction due to decoherence, thereby making the geometric phase more robust. Our work on the geometric phase should be important not only for studies of the geometric phase itself as well as its practical implementations, but also for investigating the role of system-environment correlations in open quantum systems.

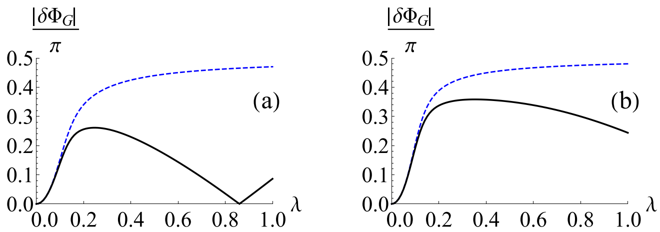

FIG. 8. Behavior of the correction to geometric phase $\delta\Phi_G = \Phi_G - \Phi_0$ (here Φ_0 is the geometric phase when the system-environment coupling strength is zero) as the spin-spin environment coupling strength λ is varied, both with (solid, black) and without (dashed, blue) initial correlations when the initial state is prepared by a unitary operation. As before, we have considered the environment to be a spin bath with $N = 50$, and $\lambda_j = \lambda$ for all j. Once again, we are working in dimensionless units with $\hbar = 1$ and here have set $\omega_i = 1$ for all i. In (a), we have used $\beta = 1$, while in (b) $\beta = 0.4$. Also, $\omega_0 = 5$ and $\Omega = e^{i\pi\sigma_y/3}$.

ACKNOWLEDGMENTS

The authors acknowledge support from the LUMS FIF Grant No. FIF-413. A.Z.C. is also grateful for support from HEC under Grant No. 5917/Punjab/NRPU/R&D/HEC/2016. Support from the National Center for Nanoscience and Nanotechnology is also acknowledged.

APPENDIX A: SOLUTION FOR HARMONIC-OSCILLATOR ENVIRONMENT

For completeness, we sketch how to solve for the system dynamics for the total system-environment Hamiltonian $H = H_S + H_B + H_{SB}$, where [53,55]

$$H_S = \frac{\omega_0}{2}\sigma_z, \quad H_B = \sum_k \omega_k b_k^\dagger b_k,$$

$$H_{SB} = \sigma_z \sum_k (g_k^* b_k + g_k b_k^\dagger).$$

First, we transform to the interaction picture to obtain

$$\begin{aligned} H_I(t) &= e^{i(H_S+H_B)t} H_{\mathrm{SB}} e^{-i(H_S+H_B)t} \\ &= \sigma_z \sum_k (g_k^* b_k e^{-i\omega_k t} + g_k b_k^\dagger e^{i\omega_k t}). \end{aligned} \tag{A1}$$

We next find the time evolution operator $U_I(t)$ corresponding to $H_I(t)$ using the Magnus expansion as

$$U_I(t) = \exp\left\{\sigma_z \sum_k [b_k^\dagger \alpha_k(t) - b_k \alpha_k^*(t)]/2\right\}, \tag{A2}$$

and the total unitary time-evolution operator is $U(t) = e^{-i\omega_0\sigma_z t/2} U_I(t)$. We now define $[\rho_S(t)]_{10} = \mathrm{Tr}_{S,B}[U(t)\rho(0)U^\dagger(t)|0\rangle\langle 1|]$. Defining $P_{01}(t) = U^\dagger(t)|0\rangle\langle 1|U(t)$, this can be written as $[\rho_S(t)]_{10} = \mathrm{Tr}_{S,B}[\rho(0)P_{01}(t)]$. Simplifying $P_{01}(t)$ using the unitary time-evolution operator $U(t)$, we find that

$$P_{01}(t) = e^{i\omega_0 t} e^{-R_{01}(t)} P_{01}, \tag{A3}$$

where

$$R_{01}(t) = \sum_k [b_k^\dagger \alpha_k(t) - b_k \alpha_k^*(t)], \tag{A4}$$

with

$$\alpha_k(t) = \frac{2g_k(1 - e^{i\omega_k t})}{\omega_k}.$$

Consequently,

$$[\rho_S(t)]_{10} = e^{i\omega_0 t}\mathrm{Tr}_{S,B}[e^{-R_{01}(t)} P_{01}\rho(0)]. \tag{A5}$$

This is a general result because it applies to an arbitrary initial density $\rho(0)$. Now, if $\rho(0) = \rho_S(0) \otimes \rho_B$, where $\rho_B = \frac{e^{-\beta H_B}}{Z_B}$ with $Z_B = \mathrm{Tr}_B[e^{-\beta H_B}]$, then

$$[\rho_S(t)]_{10} = [\rho_S(0)]_{10} e^{i\omega_0 t}\mathrm{Tr}_B[e^{-R_{01}(t)}\rho_B]. \tag{A6}$$

The trace over the environment computes to

$$\begin{aligned} &\mathrm{Tr}_B[e^{-R_{01}(t)}\rho_B] \\ &= \exp\left[-\sum_k 4|g_k|^2 \frac{[1-\cos(\omega_k t)]}{\omega_k^2}\coth\left(\frac{\beta\omega_k}{2}\right)\right], \end{aligned} \tag{A7}$$

thereby yielding

$$[\rho_S(t)]_{10} = [\rho_S(0)]_{10} e^{i\omega_0 t} e^{-\Gamma_{\mathrm{uc}}(t)}, \tag{A8}$$

with

$$\Gamma_{\mathrm{uc}}(t) = \sum_k 4|g_k|^2 \frac{[1-\cos(\omega_k t)]}{\omega_k^2}\coth\left(\frac{\beta\omega_k}{2}\right). \tag{A9}$$

We now consider what happens if the initial state is of the form $\rho(0) = \frac{1}{Z}\Omega\, e^{-\beta H}\Omega^\dagger$, with Z the normalization factor. Currently, the Ω operator can be a projection operator or a unitary operator. To first simplify Z, we use the completeness relation $\sum_l |l\rangle\langle l| = \mathbb{1}$, where $\sigma_z|l\rangle = (-1)^l|l\rangle$. Then,

$$Z = \sum_l e^{-\beta\omega_0(-1)^l/2}\langle l|\Omega^\dagger\Omega|l\rangle \mathrm{Tr}_B\big[e^{-\beta H_B^{(l)}}\big], \tag{A10}$$

with

$$H_B^{(l)} = H_B + (-1)^l \sum_k (g_k^* b_k + g_k b_k^\dagger). \tag{A11}$$

To simplify further, we introduce the displaced harmonic-oscillator modes

$$B_{k,l} = b_k + \frac{(-1)^l g_k}{\omega_k}, \tag{A12}$$

$$B_{k,l}^\dagger = b_k^\dagger + \frac{(-1)^l g_k^*}{\omega_k}, \tag{A13}$$

allowing us to write

$$Z = \sum_l e^{-\beta\omega_0(-1)^l/2}\langle l|\Omega^\dagger\Omega|l\rangle e^{\beta\sum_k \frac{|g_k|^2}{\omega_k}} Z_B, \tag{A14}$$

where $Z_B = \mathrm{Tr}_B[e^{-\beta\sum_k \omega_k B_{k,l}^\dagger B_{k,l}}]$. With Z found, we then substitute our initial state in Eq. (A5) and introduce $\sum_l |l\rangle\langle l|$ to simplify the resulting $\mathrm{Tr}_B[e^{-R_{01}(t)}e^{-\beta H_B^{(l)}}]$. Using the displaced harmonic-oscillator modes as before, we find that

$$R_{01}(t) = \sum_k [\alpha_k(t)B_{k,l}^\dagger - \alpha_k^*(t)B_{k,l}] + i(-1)^l\Phi(t), \tag{A15}$$

where

$$\Phi(t) = \sum_k \frac{4|g_k|^2}{\omega_k^2} \sin(\omega_k t). \tag{A16}$$

We then find that

$$\mathrm{Tr}_B\big[e^{-R_{01}(t)} e^{-\beta H_B^{(l)}}\big] = e^{-i(-1)^l \Phi(t)} Z_B e^{\beta \sum_k \frac{|g_k|^2}{\omega_k}} e^{-\Gamma_{\mathrm{uc}}(t)}. \tag{A17}$$

Putting this all together, and rearranging, we obtain

$$[\rho_S(t)]_{10} = [\rho_S(0)]_{10} e^{i\omega_0 t} e^{-\Gamma_{\mathrm{uc}}(t)} X(t), \tag{A18}$$

with

$$X(t) = \frac{\sum_l \langle l|\Omega^\dagger P_{01}\Omega|l\rangle e^{-i(-1)^l\Phi(t)} e^{-\beta\omega_0(-1)^l/2}}{\sum_l \langle l|\Omega^\dagger P_{01}\Omega|l\rangle e^{-\beta\omega_0(-1)^l/2}}.$$

Assuming that Ω is a projection operator, that is, $\Omega = |\psi\rangle\langle\psi|$, we can further simplify and write $X(t)$ in polar form to obtain Eq. (18). On the other hand, if Ω is taken to be a unitary operator, we obtain Eq. (23).

Now, to actually calculate the density matrix for the central two-level system, we need to calculate the sums involved in the evaluation of $\Gamma_{\mathrm{uc}}(t)$ and $\Phi(t)$. As mentioned in the main text, these sums are performed by converting the sums to integrals via $\sum_k 4|g_k|^2(\dots) \to \int_0^\infty d\omega\, J(\omega)(\dots)$, where $J(\omega)$ is the spectral density. Assuming that $J(\omega) = \lambda\omega^s\omega_c^{1-s}e^{-\omega/\omega_c}$, the integrals can be performed analytically. For $\Phi(t)$, we find that

$$\Phi(t) = \frac{\lambda\Gamma(s-1)}{\left(1+\omega_c^2t^2\right)^{(s-1)/2}} \sin[(s-1)\arctan(\omega_c t)], \tag{A19}$$

for $s > 0$ and $s \neq 1$. On the other hand, for $s = 1$,

$$\Phi(t) = \lambda \arctan(\omega_c t). \tag{A20}$$

For $\Gamma_{\mathrm{uc}}(t)$, we can split this decoherence factor into two parts. One part, labeled as $\Gamma_{\mathrm{vac}}(t)$, is only due to the vacuum fluctuations, and hence is nonzero even at zero temperature. The other part, namely $\Gamma_{\mathrm{th}}(t)$, is nonzero only at nonzero temperatures. In other words, we have

$$\Gamma_{\mathrm{uc}}(t) = \Gamma_{\mathrm{vac}}(t) + \Gamma_{\mathrm{th}}(t), \tag{A21}$$

$$\Gamma_{\mathrm{vac}}(t) = \int_0^\infty d\omega\, J(\omega)\frac{1-\cos\omega t}{\omega^2}, \tag{A22}$$

$$\Gamma_{\mathrm{th}}(t) = \int_0^\infty d\omega\, J(\omega)[\coth(\beta\omega/2) - 1]\frac{1-\cos\omega t}{\omega^2}. \tag{A23}$$

For $J(\omega) = \lambda\omega^s\omega_c^{1-s}e^{-\omega/\omega_c}$, we find that

$$\Gamma_{\mathrm{vac}}(t) = \lambda\Gamma(s-1)\left(1 - \frac{\cos[(s-1)\arctan(\omega_c t)]}{\left(1+\omega_c^2t^2\right)^{(s-1)/2}}\right), \tag{A24}$$

for $s \neq 1$. For $s = 1$,

$$\Gamma_{\mathrm{vac}}(t) = \frac{\lambda}{2}\ln\left(1+\omega_c^2t^2\right). \tag{A25}$$

Finally, $\Gamma_{\mathrm{th}}(t)$ for $s \neq 1$ is given by

$$\Gamma_{\mathrm{th}}(t) = 2\lambda(\omega_c\beta)^{1-s}\,\Gamma(s-1)\sum_{k=1}^\infty \frac{1}{(k+1/\omega_c\beta)^{s-1}} \times \left\{1 - \left[1 + \frac{(t/\beta)^2}{(k+1/\omega_c\beta)^2}\right]^{-(s-1)/2} \cos[(s-1)\phi_k(t)]\right\}, \tag{A26}$$

where $\phi_k(t) = \arctan\left(\frac{t/\beta}{k+1/\omega_c\beta}\right)$. On the other hand, for $s = 1$,

$$\Gamma_{\mathrm{th}}(t) = 2\lambda[\ln\Gamma(1+1/\omega_c\beta) - \tfrac{1}{2}\ln|\Gamma(1+1/\omega_c\beta + it/\beta)|^2]. \tag{A27}$$

APPENDIX B: GEOMETRIC PHASE CORRECTION VIA AN EFFECTIVE MAGNETIC FIELD

As explained in the main text, if the system-environment interactions are taken into account, the initial state of the environment is a collection of displaced harmonic oscillators. These displaced harmonic oscillators then not only lead to the decoherence of the central two-level system, but also lead to an additional phase shift of the two-level system $\chi(t)$. In other words, the displaced harmonic oscillators "produce" an additional effective magnetic field $B(t) = \frac{d\chi}{dt}$ for the two-level system to interact with. To see the effect of this effective magnetic field in an alternate way, suppose that the system-environment Hamiltonian is

$$H = \frac{\omega_0}{2}\sigma_z + \frac{B(t)}{2}\sigma_z + \sum_k \omega_k b_k^\dagger b_k + \sigma_z\sum_k (g_k^* b_k + g_k b_k^\dagger), \tag{B1}$$

and the initial system state is $\rho_S(0)\otimes e^{-\beta H_B}/Z_B$. In other words, the effect of the displaced harmonic oscillators is incorporated from the start via $B(t)$. We can then argue that, for particular forms of $B(t)$, the correction to the geometric phase becomes very small. To show that this effective magnetic-field approach is able to reproduce the geometric phase, let us look at the sub-Ohmic case in detail. For small values of s, we find that the effective magnetic field is approximately $B(t) \approx -\lambda\Gamma(s-1)\omega_c$. Then, using this in Eq. (B1), we can work out the dynamics of the two-level system with this effective Hamiltonian, and hence the geometric phase. The results are shown in Fig. 9(a). The dashed red curve shows the geometric phase with the effective magnetic field $B(t) \approx -\lambda\Gamma(s-1)\omega_c$, while the solid black curve is the geometric phase using the exact dynamics. It is clear that, for small values of s, the agreement is excellent; for larger values with sub-Ohmic environments, the effective field is no longer linear, leading to the discrepancy.

Similarly, we can also work out the correction to the geometric phase for super-Ohmic environments using the effective Hamiltonian Eq. (B1), except that the effective magnetic field is now given by approximately

$$B(t) = \lambda\Gamma(s-1)\omega_c(s-1)e^{-t/\bar{\tau}}\cos[(s-1)\omega_c t],$$

with $\bar{\tau} = \frac{1}{\omega_c}\tan\left[\frac{\pi}{s}\right]$. That is, the effective magnetic field is now an oscillatory, decaying function. Results are illustrated

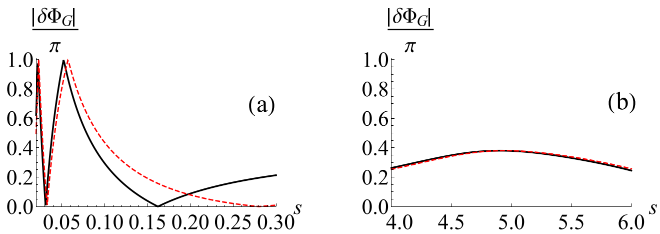

FIG. 9. Behavior of the correction to the geometric phase $\delta\Phi_G = \Phi_G - \Phi_U$ with the exact dynamics (the solid-black line) and the approximate effective magnetic field $B(t) \approx -\lambda\Gamma(s-1)\omega_c$ (dashed, red curve) for sub-Ohmic environments [see (a)], and the effective magnetic field $B(t) \approx \lambda\Gamma(s-1)\omega_c(s-1)e^{-t/\bar{\tau}}\cos[(s-1)\omega_c t]$ (dashed, red curve) for super-Ohmic environments [see (b)]. As always, we are working in dimensionless units with $\hbar = 1$ and here we have set $\omega_0 = 1$. Also, $\theta_0 = \pi/3$, $\omega_c = 5$, $\lambda = 0.4$, and $\beta \to \infty$.

in Fig. 9(b). As expected, the effective field approach is able to capture the exact behavior of the geometric phase very well.

APPENDIX C: DYNAMICS WITH A SPIN ENVIRONMENT

We now consider the total system-environment Hamiltonian $H = H_S + H_B + H_{SB}$, where

$$H_S = \frac{\omega_0}{2}\sigma_z, \quad H_B = \sum_i \omega_i\sigma_x^i, \quad H_{SB} = \sigma_z \otimes \sum_i \lambda_i\sigma_z^i.$$

Once again, since $[H_S, H_{SB}] = 0$, this is a pure dephasing model. Our aim is to then calculate $\langle\sigma_\pm(t)\rangle$. We note that $e^{it(H_B+H_{SB})}|l\rangle = e^{it[H_B+(-1)^l V]}|l\rangle$, where

$$V = \sum_i \lambda_i\sigma_z^i. \tag{C1}$$

Using the completeness relation $\sum_s |l\rangle\langle l| = \mathbb{1}$, we can simplify $\sigma_\pm(t) = e^{iHt}\sigma_\pm e^{-iHt}$ to find

$$\sigma_\pm(t) = e^{\pm i\omega_0 t}e^{it(H_B\pm V)}e^{-it(H_B\mp V)}\sigma_\pm. \tag{C2}$$

We now consider initial states of the form

$$\rho(0) = \rho_S(0)\otimes\rho_B, \quad \rho_B = e^{-\beta H_B}/Z_B. \tag{C3}$$

For simplicity, we only show the calculation for $\langle\sigma_+(t)\rangle$. Using Eq. (C2), we obtain

$$\langle\sigma_+(t)\rangle = \text{Tr}[\sigma_+(t)\rho(0)] = \frac{e^{i\omega_0 t}}{Z_B}\langle\sigma_+(0)\rangle\text{Tr}_B[R(t)e^{-\beta H_B}], \tag{C4}$$

where $R(t) = e^{it(H_B+V)}e^{-it(H_B-V)}$. Our remaining task is to compute $\text{Tr}_B[R(t)e^{-\beta H_B}]$. To this end, we first write $R(t)$ as $e^{it\sum_j\alpha_j(\vec{n}_1^j\cdot\vec{\sigma}_j)}e^{-it\sum_j\alpha_j(\vec{n}_2^j\cdot\vec{\sigma}_j)}$, where $\vec{n}_1^j = \frac{1}{\alpha_j}(\omega_j, 0, \lambda_j)$, $\vec{n}_2^j = \frac{1}{\alpha_j}(\omega_j, 0, -\lambda_j)$, and $\alpha_j = \sqrt{\omega_j^2 + \lambda_j^2}$. The exponentials can then be combined and the resulting expression is further simplified to obtain

$$\text{Tr}_B[R(t)e^{-\beta H_B}] = 2^N\prod_j \cos c_j\cos(i\beta\omega_j), \tag{C5}$$

where $\cos c_j = 1 - 2\left(\frac{\lambda_j}{\alpha_j}\right)^2\sin^2(\alpha_j t)$ and $Z_B = 2^N\prod_j\cos(i\beta\omega_j)$. Putting it all together, we finally have that

$$\langle\sigma_+(t)\rangle = \langle\sigma_+(0)\rangle e^{i\omega_0 t}\prod_j\left\{1 - 2\left(\frac{\lambda_j}{\alpha_j}\right)^2\sin^2(\alpha_j t)\right\}. \tag{C6}$$

We now consider initially correlated states of the form

$$\rho(0) = \frac{1}{Z}\Omega\, e^{-\beta H}\Omega^\dagger.$$

As before, we find that $\langle\sigma_+(t)\rangle = \text{Tr}_{S,B}[e^{i\omega_0 t}R(t)\sigma_+\rho(0)]$. To simplify $\rho(0)$, we use the fact that $e^{-\beta H}|s\rangle = e^{(-1)^{s+1}\beta\omega_0/2}e^{-\beta[H_B+(-1)^s V]}|s\rangle$. We then have

$$\langle\sigma_+(t)\rangle = \frac{e^{i\omega_0 t}}{Z}[\langle 0|\Omega^\dagger\sigma_+\Omega|0\rangle e^{-\beta\omega_0/2}\text{Tr}_B[R(t)e^{-\beta(H_B+V)}] + \langle 1|\Omega^\dagger\sigma_+\Omega|1\rangle e^{\beta\omega_0/2}\text{Tr}_B[R(t)e^{-\beta(H_B-V)}]]. \tag{C7}$$

We now sketch the calculation for $\text{Tr}_B[R(t)e^{-\beta(H_B+V)}]$ as the calculation for $\text{Tr}_B[R(t)e^{-\beta(H_B-V)}]$ is very similar. The trick is to write $\text{Tr}_B[R(t)e^{-\beta(H_B+V)}]$ as $\text{Tr}_B[e^{-it(H_B-V)}e^{i\gamma(H_B+V)}]$ we have defined $\gamma = t + i\beta$. The exponentials can then be manipulated as before to obtain

$$\text{Tr}_B[R(t)e^{-\beta(H_B+V)}] = C_0\Pi_j(A_j - iB_j),$$

where $A_j = 1 - 2(\frac{\lambda_j}{\alpha_j})^2\sin^2(\alpha_j t)$, $B_j = 2(\frac{\lambda_j}{\alpha_j})^2\tanh(\beta\alpha_j)\sin(\alpha_j t)\cos(\alpha_j t)$, and $C_0 = \Pi_j 2\cosh(\beta\alpha_j)$. We can then further simplify to

$$\langle\sigma_+(t)\rangle = \langle\sigma_+\rangle e^{i\omega_0 t}e^{-\Gamma(t)} \times \frac{\sum_l\langle l|\Omega^\dagger\sigma_+\Omega|l\rangle e^{-\beta\omega_0(-1)^l/2}e^{-i(-1)^l\Phi(t)}}{\sum_l\langle l|\Omega^\dagger\sigma_+\Omega|l\rangle e^{-\beta\omega_0(-1)^l/2}},$$

where

$$\Gamma(t) = \sum_j\Gamma_j(t), \quad \Phi(t) = \sum_j\Phi_j(t), \tag{C8}$$

and $F_j(t) = A_j(t) + iB_j(t) = e^{-\Gamma_j(t)}e^{i\Phi_j(t)}$. It is then a simple matter of specifying that Ω is a projection operator or a unitary operator to work out the dynamics.

[1] E. Sjoqvist, Geometric phases in quantum information, Int. J. Quantum Chem. **115**, 1311 (2015).

[2] E. Cohen, H. Larocque, F. Bouchard, F. Nejadsattari, Y. Gefen, and E. Karimi, Geometric phase from Aharonov-Bohm to Pancharatnam-Berry and beyond, Nat. Rev. Phys. **1**, 437 (2019).

[3] S. Pancharatnam, Generalized theory of interference and its applications, Proc. Indian Acad. Sci. A **44**, 398 (1956).

[4] H. Longuet-Higgins, The intersection of potential energy surfaces in polyatomic molecules, Proc. R. Soc. London A **344**, 147 (1975).

[5] A. J. Stone, Spin-orbit coupling and the intersection of potential energy surfaces in polyatomic molecules, Proc. R. Soc. London A **351**, 141 (1976).

[6] M. V. Berry, Quantal phase factors accompanying adiabatic changes, Proc. R. Soc. London A **392**, 45 (1984).

[7] Y. Aharonov and J. Anandan, Phase Change During a Cyclic Quantum Evolution, Phys. Rev. Lett. **58**, 1593 (1987).

[8] A. Uhlmann, On Berry phases along mixtures of states, Ann. Phys. (NY) **501**, 63 (1989).

[9] E. Sjöqvist, A. K. Pati, A. Ekert, J. S. Anandan, M. Ericsson, D. K. L. Oi, and V. Vedral, Geometric Phases for Mixed States in Interferometry, Phys. Rev. Lett. **85**, 2845 (2000).

[10] D. Suter, G. Chingas, R. Harris, and A. Pines, Berry's phase in magnetic resonance, Mol. Phys. **61**, 1327 (1987).

[11] P. J. Leek, J. M. Fink, A. Blais, R. Bianchetti, M. Göppl, J. M. Gambetta, D. I. Schuster, L. Frunzio, R. J. Schoelkopf, and A. Wallraff, Observation of Berry's phase in a solid-state qubit, Science **318**, 1889 (2007).

[12] R. Simon, H. J. Kimble, and E. C. G. Sudarshan, Evolving Geometric Phase and its Dynamical Manifestation as a Frequency Shift: An Optical Experiment, Phys. Rev. Lett. **61**, 19 (1988).

[13] S.-L. Zhu, Scaling of Geometric Phases Close to the Quantum Phase Transition in the *xy* Spin Chain, Phys. Rev. Lett. **96**, 077206 (2006).

[14] L. Campos Venuti and P. Zanardi, Quantum Critical Scaling of the Geometric Tensors, Phys. Rev. Lett. **99**, 095701 (2007).

[15] P. Zanardi and M. Rasetti, Holonomic quantum computation, Phys. Lett. A **264**, 94 (1999).

[16] J. A. Jones, V. Vedral, A. Ekert, and G. Castagnoli, Geometric quantum computation using nuclear magnetic resonance, Nature (London) **403**, 869 (2000).

[17] G. Falci, R. Fazio, G. Massimo Palma, J. Siewert, and V. Vedral, Detection of geometric phases in superconducting nanocircuits, Nature (London) **407**, 355 (2000).

[18] L.-M. Duan, J. I. Cirac, and P. Zoller, Geometric manipulation of trapped ions for quantum computation, Science **292**, 1695 (2001).

[19] W. X.-Bin and M. Keiji, Nonadiabatic Conditional Geometric Phase Shift with NMR, Phys. Rev. Lett. **87**, 097901 (2001).

[20] D. Liebfried, B. DeMarco, V. Meyer, D. Lucas, M. Barrett, J. Britton, W. M. Itano, B. Jelenkovic, C. Langer, T. Rosenband, and D. J. Wineland, Experimental demonstration of a robust, high-fidelity geometric two ion-qubit phase gate, Nature (London) **422**, 412 (2000).

[21] M. Ericsson, E. Sjöqvist, J. Brännlund, D. K. L. Oi, and A. K. Pati, Generalization of the geometric phase to completely positive maps, Phys. Rev. A **67**, 020101(R) (2003).

[22] A. Carollo, I. Fuentes-Guridi, M. F. Santos, and V. Vedral, Geometric Phase in Open Systems, Phys. Rev. Lett. **90**, 160402 (2003).

[23] D. M. Tong, E. Sjöqvist, L. C. Kwek, and C. H. Oh, Kinematic Approach to the Mixed State Geometric Phase in Nonunitary Evolution, Phys. Rev. Lett. **93**, 080405 (2004).

[24] R. S. Whitney, Y. Makhlin, A. Shnirman, and Y. Gefen, Geometric Nature of the Environment-Induced Berry Phase and Geometric Dephasing, Phys. Rev. Lett. **94**, 070407 (2005).

[25] X. X. Yi, D. M. Tong, L. C. Wang, L. C. Kwek, and C. H. Oh, Geometric phase in open systems: Beyond the Markov approximation and weak-coupling limit, Phys. Rev. A **73**, 052103 (2006).

[26] F. C. Lombardo and P. I. Villar, Geometric phases in open systems: A model to study how they are corrected by decoherence, Phys. Rev. A **74**, 042311 (2006).

[27] J. Dajka, M. Mierzejewski, and J. Łuczka, Geometric phase of a qubit in dephasing environments, J. Phys. A **41**, 012001 (2008).

[28] F. C. Lombardo and P. I. Villar, Environmentally induced effects on a bipartite two-level system: Geometric phase and entanglement properties, Phys. Rev. A **81**, 022115 (2010).

[29] F. M. Cucchietti, J.-F. Zhang, F. C. Lombardo, P. I. Villar, and R. Laflamme, Geometric Phase with Nonunitary Evolution in the Presence of a Quantum Critical Bath, Phys. Rev. Lett. **105**, 240406 (2010).

[30] P. I. Villar and F. C. Lombardo, Geometric phases in the presence of a composite environment, Phys. Rev. A **83**, 052121 (2011).

[31] F. C. Lombardo and P. I. Villar, Nonunitary geometric phases: A qubit coupled to an environment with random noise, Phys. Rev. A **87**, 032338 (2013).

[32] F. C. Lombardo and P. I. Villar, Correction to the geometric phase by structured environments: The onset of non-Markovian effects, Phys. Rev. A **91**, 042111 (2015).

[33] A. Carollo, B. Spagnolo, and D. Valenti, Uhlmann curvature in dissipative phase transitions, Sci. Rep. **8**, 9852 (2018).

[34] A. Carollo, B. Spagnolo, and D. Valenti, Symmetric logarithmic derivative of fermionic Gaussian states, Entropy **20**, 485 (2018).

[35] V. Hakim and V. Ambegaokar, Quantum theory of a free particle interacting with a linearly dissipative environment, Phys. Rev. A **32**, 423 (1985).

[36] F. Haake and R. Reibold, Strong damping and low-temperature anomalies for the harmonic oscillator, Phys. Rev. A **32**, 2462 (1985).

[37] H. Grabert, P. Schramm, and G.-L. Ingold, Quantum Brownian motion: The functional integral approach, Phys. Rep. **168**, 115 (1988).

[38] C. M. Smith and A. O. Caldeira, Application of the generalized Feynman-Vernon approach to a simple system: The damped harmonic oscillator, Phys. Rev. A **41**, 3103 (1990).

[39] R. Karrlein and H. Grabert, Exact time evolution and master equations for the damped harmonic oscillator, Phys. Rev. E **55**, 153 (1997).

[40] L. D. Romero and J. P. Paz, Decoherence and initial correlations in quantum Brownian motion, Phys. Rev. A **55**, 4070 (1997).

[41] E. Lutz, Effect of initial correlations on short-time decoherence, Phys. Rev. A **67**, 022109 (2003).

[42] S. Banerjee and R. Ghosh, General quantum Brownian motion with initially correlated and nonlinearly coupled environment, Phys. Rev. E **67**, 056120 (2003).

[43] N. G. van Kampen, A new approach to noise in quantum mechanics, J. Stat. Phys. **115**, 1057 (2004).

[44] M. Ban, Quantum master equation for dephasing of a two-level system with an initial correlation, Phys. Rev. A **80**, 064103 (2009).

[45] M. Campisi, P. Talkner, and P. Hänggi, Fluctuation Theorem for Arbitrary Open Quantum Systems, Phys. Rev. Lett. **102**, 210401 (2009).

[46] C. Uchiyama and M. Aihara, Role of initial quantum correlation in transient linear response, Phys. Rev. A **82**, 044104 (2010).

[47] A. G. Dijkstra and Y. Tanimura, Non-Markovian Entanglement Dynamics in the Presence of System-Bath Coherence, Phys. Rev. Lett. **104**, 250401 (2010).

[48] A. Smirne, H.-P. Breuer, J. Piilo, and B. Vacchini, Initial correlations in open-systems dynamics: The Jaynes-Cummings model, Phys. Rev. A **82**, 062114 (2010).
[49] J. Dajka and J. Łuczka, Distance growth of quantum states due to initial system-environment correlations, Phys. Rev. A **82**, 012341 (2010).
[50] Y.-J. Zhang, X.-B. Zou, Y.-J. Xia, and G.-C. Guo, Different entanglement dynamical behaviors due to initial system-environment correlations, Phys. Rev. A **82**, 022108 (2010).
[51] H.-T. Tan and W.-M. Zhang, Non-Markovian dynamics of an open quantum system with initial system-reservoir correlations: A nanocavity coupled to a coupled-resonator optical waveguide, Phys. Rev. A **83**, 032102 (2011).
[52] C. K. Lee, J. Cao, and J. Gong, Noncanonical statistics of a spin-boson model: Theory and exact Monte Carlo simulations, Phys. Rev. E **86**, 021109 (2012).
[53] V. G. Morozov, S. Mathey, and G. Röpke, Decoherence in an exactly solvable qubit model with initial qubit-environment correlations, Phys. Rev. A **85**, 022101 (2012).
[54] V. Semin, I. Sinayskiy, and F. Petruccione, Initial correlation in a system of a spin coupled to a spin bath through an intermediate spin, Phys. Rev. A **86**, 062114 (2012).
[55] A. Z. Chaudhry and J. Gong, Amplification and suppression of system-bath-correlation effects in an open many-body system, Phys. Rev. A **87**, 012129 (2013).
[56] A. Z. Chaudhry and J. Gong, Role of initial system-environment correlations: A master equation approach, Phys. Rev. A **88**, 052107 (2013).
[57] A. Z. Chaudhry and J. Gong, The effect of state preparation in a many-body system, Can. J. Chem. **92**, 119 (2013).
[58] J. Reina, C. Susa, and F. Fanchini, Extracting information from qubit-environment correlations, Sci. Rep. **4**, 7443 (2014).
[59] Y.-J. Zhang, W. Han, Y.-J. Xia, Y.-M. Yu, and H. Fan, Role of initial system-bath correlation on coherence trapping, Sci. Rep. **5**, 13359 (2015).
[60] C.-C. Chen and H.-S. Goan, Effects of initial system-environment correlations on open-quantum-system dynamics and state preparation, Phys. Rev. A **93**, 032113 (2016).
[61] I. de Vega and D. Alonso, Dynamics of non-Markovian open quantum systems, Rev. Mod. Phys. **89**, 015001 (2017).
[62] J. C. Halimeh and I. de Vega, Weak-coupling master equation for arbitrary initial conditions, Phys. Rev. A **95**, 052108 (2017).
[63] S. Kitajima, M. Ban, and F. Shibata, Expansion formulas for quantum master equations including initial correlation, J. Phys. A **50**, 125303 (2017).
[64] M. Buser, J. Cerrillo, G. Schaller, and J. Cao, Initial system-environment correlations via the transfer-tensor method, Phys. Rev. A **96**, 062122 (2017).
[65] M. Majeed and A. Z. Chaudhry, Effect of initial system-environment correlations with spin environments, Eur. Phys. J. D **73**, 16 (2019).
[66] H.-P. Breuer and F. Petruccione, *The Theory of Open Quantum Systems* (Oxford University Press, Oxford, 2007).
[67] U. Weiss, *Quantum Dissipative Systems* (World Scientific, Singapore, 2008).
[68] F. M. Cucchietti, J. P. Paz, and W. H. Zurek, Decoherence from spin environments, Phys. Rev. A **72**, 052113 (2005).
[69] S. Camalet and R. Chitra, Effect of random interactions in spin baths on decoherence, Phys. Rev. B **75**, 094434 (2007).
[70] M. Schlosshauer, *Decoherence and the Quantum-to-Classical Transition* (Springer, Berlin, 2007).
[71] P. I. Villar, Spin bath interaction effects on the geometric phase, Phys. Lett. A **373**, 206 (2009).